

Role of Magnetic Resonance Imaging for Evaluation of Cardiac Masses

Berroho O*, Saidi S, Lamliki O, Doghmi N, Cherti M

Cardiology B department, Ibn Sina University Hospital, Rabat, Morocco

*Corresponding author: Berroho O

| Received: 04.03.2019 | Accepted: 15.03.2019 | Published: 30.03.2019

DOI: [10.36347/sjams.2019.v07i03.093](https://doi.org/10.36347/sjams.2019.v07i03.093)

Abstract

Review Article

Cardiac tumors benign and malignant are rare. However, when there is clinical suspicion, proper diagnostic evaluation is necessary to plan the most appropriate treatment. The therapeutic management differs fundamentally according to the nature of the cardiac mass and tumor type, and depends on clinical circumstances such as hemodynamic failure, invasive growth, and metastatic spreading, which either prompt for an intervention or rather make it irrational. (1,2) The imaging method most frequently used to assess a suspicious cardiac lesion is the transthoracic echocardiogram (TTE). (2,3) However, in the last few years, cardiovascular magnetic resonance imaging (CMRI) has been established as the gold standard for imaging and evaluation of cardiac masses. (4) CMRI is a non-invasive technique, does not use ionizing radiation, has a wide field of view and provides high contrast resolution and also allows the evaluation of cardiac morphology, tissue property and function in a single exam. (5)

Keywords: CMRI, cardiac masses.

Copyright © 2019: This is an open-access article distributed under the terms of the Creative Commons Attribution license which permits unrestricted use, distribution, and reproduction in any medium for non-commercial use (NonCommercial, or CC-BY-NC) provided the original author and source are credited.

INTRODUCTION

Cardiac tumors are rare but important cause of morbidity and mortality [1, 2, 6], they affect patients of all ages with an estimated prevalence of only 0.0017 and 0.19% in autopsy series [7], they may be neoplastic or non-neoplastic.

Approximately 75% of all primary cardiac tumors are benign histologically, and the remainder are malignant, the most common of the benign cardiac tumors in the adult population are myxomas (52%), other less common benign tumors include papillary fibroelastomas (16%), lipomas (16%), hemangiomas (6%), fibromas (3%) and rhabdomyomas (1%) [8, 9].

The most prevalent primary malignant tumors are the cardiac sarcomas. Metastases involving the heart and pericardium are more common than primary cardiac tumors, and 15% of patients with any type of cancer may present with cardiac metastases [10, 11].

Among the differential diagnoses for neoplasia, intracardiac thrombus [12] is highlighted. Cardiac tumors are usually asymptomatic and often discovered incidentally during evaluation of an unrelated problem or physical finding. [14-16].

Advances in cardiac imaging greatly facilitate the diagnosis and management of cardiac tumors, although transthoracic echocardiography is useful in the

initial evaluation for screening. In their further evaluation, cardiac magnetic resonance (CMR) imaging has become a greatly valuable technique and the imaging modality of choice for their assessment [17]. In this article we review the role of MR imaging in the assessment of cardiac masses. We provide a detailed description of a core protocol for the MR assessment of cardiac masses and tumors and illustrate the different imaging characteristics of the most common types of mass, with case examples.

Cardiac MRI sequences

A wide variety of cardiac MRI pulse sequences can be used to confirm the presence of a suspected cardiac mass and help characterize its tissue composition and impact on adjacent structures. The differentiation of normal from abnormal tissue on CMRI is based on intrinsic differences in hydrogen proton density and T1-T2 relaxation properties of the relevant tissues. Consequently, T1 and T2 weighted images are used to delineate the morphology and anatomy relevant to the diagnosis of cardiac tumors. Malignant cells have generally more free intracellular water content and a higher degree of surrounding extracellular fluid due to interstitial oedema and hence a longer T1 and T2 relaxation times compared with benign pathology [18]. Malignant tissue is associated with a greater degree of neo-angiogenesis and hence first pass contrast enhancement. Necrotic tumour tissue is associated with interstitial expansion

with accumulation and delayed washout of contrast agents [19].

Black blood techniques

Black-blood static MRI images are used to help localise a suspected cardiac or para cardiac mass and to infer the tissue composition of a mass. They are classically obtained using a double-inversion recovery fast spin-echo sequence. The first 180° inversion pulse is non slice selective and inverts magnetization within the entire tissue volume.

This is immediately followed by a slice-selective 180° pulse. This causes blood flowing into the slice to undergo only the first non selective 180° inversion pulse giving it a black-blood appearance. To achieve T1-weighted images the time to repeat (TR) is set at around 1000 ms; T2-weighted images require a TR of around 2000 ms which necessitates sampling every other RR interval and hence double the acquisition time. The addition of a third slice selective 180° inversion pulse (triple inversion recovery) can be used to provide fat saturation which is especially helpful for characterisation of a fat containing lesion such as lipoma [20].

Bright blood techniques

Ciné steady-state free precession (SSFP) sequences are used for cine imaging of the heart, which enables assessment of the mobility of a mass, its functional impact on valves, as well as delineation of an attachment point. SSFP is an un-enhanced fast gradient echo technique which uses a short TR (2-3 msec) and segmented k-space filling, enables cine cardiac imaging at high temporal resolution and at the same time gives excellent contrast definition between the blood pool and myocardium. SSFP should not be used for assessment

of tissue composition of a cardiac mass as its tissue weighting is dependent on both T1 and T2 effects [21].

First pass perfusion and delayed enhancement imaging

Gadolinium-enhanced First pass rest perfusion using a fast T1-weighted gradient echo sequence followed by 10-15 minutes delayed enhancement imaging is also used to assess lesion vascularity and composition. First pass enhancement is typical characteristic of highly vascular tumours, such as haemangioma or angiosarcoma. The presence of late phase gadolinium enhancement (LGE) suggest delayed washout from a lesion, commonly as the result of extracellular space expansion or necrosis [22].

LGE can be detecting with both benign and malignant lesions. Benign tumours like fibroma usually display uniform LGE whereas tumours with a more heterogeneous composition like myxoma or angiosarcoma usually show patchy LGE [23].

Benign tumors

A/myxoma: (figure 1)

Cardiac myxoma (CM) is by far the most common primary benign cardiac tumor and is believed to originate from pluripotent mesenchymal cells within the endocardium [24], typically arising in the left atrium with an attachment point in the fossa ovalis region. Left atrial myxomas usually present with symptoms of intermittent mitral valve obstruction, including dyspnoea and orthopnoea related to pulmonary oedema. Clinical symptoms may relate to intracardiac obstruction, systemic embolism or a systemic inflammatory response [25]. Surgical resection on time of myxoma is advocated for definite diagnosis and to reduce the risk of complications [26].

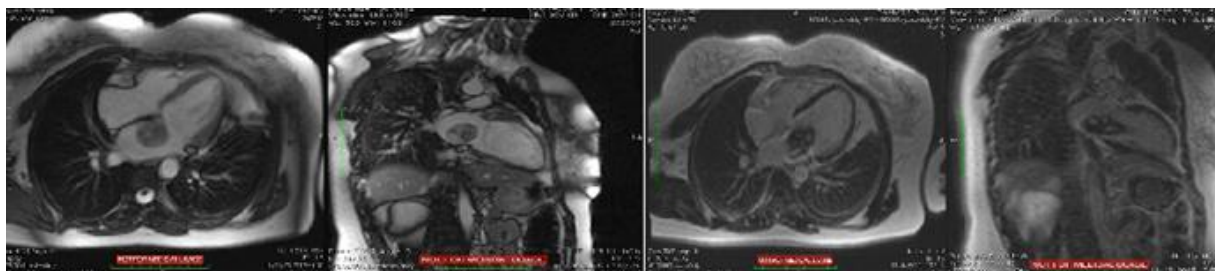


Fig-1: Cardiac MRI 4 and 2 chambers view demonstrating a large (31*27), hypointense, lobulated, left atrial mass attached to the interatrial septum and that prolapses into the left ventricle

Typical MRI features are a well-defined, smooth, spherical or ovoid mobile lobulated (figure 1) mass within either atrium, prolapsing through the atrioventricular valve orifice in diastole. Steady-state free precession (SSFP) cine imaging sequences, acquired in standard cardiac imaging planes, provide an accurate assessment of the location, attachment site and functional impact of myxomas. On cine SSFP sequences, they usually appear hyperintense compared with normal myocardium and hypointense compared with the blood pool [27]. T1 and T2-weighted images

usually show a heterogeneous appearance because of the different composition of myxoid tissue, fibrous tissue, blood and haemorrhagic breakdown products contained within myxomas [28]. Fluoroscopically visible calcification may be seen in up to 10% of all myxomas and is most commonly identified in lesions located in the right atrium [29], First pass perfusion is usually absent and LGE (Late gadolinium enhancement) is often multifocal and patchy.

B/papillary fibroelastoma

Cardiac papillary Fibroelastomas are the most common tumors of the heart valves, accounting for approximately 8% of primary benign cardiac tumors and are usually slow growing which manifest after several years [30]. At present, papillary fibroelastomas are classically discovered with echocardiography, which demonstrates a small (<1.5cm), mobile, pedunculated, homogeneous valvular or endocardial mass that flutters or prolapses with cardiac motion. On MRI, imaging are those of a hypointense well circumscribed mobile valve nodule on SSFP sequences, often with peri-lesional flow artifact [31]. T1 and T2 weighted images reflect their fibroelastic composition with uniform intermediate signal intensity similar to myocardium.

C/hemangioma :(fig.2)

Cardiac hemangiomas are benign cardiac tumors that account for 5–10% of all benign tumors of the heart. They occur in any cardiac location, including the pericardial space [32]. They are classified histologically into three types: cavernous, capillary, vessels and arteriovenous type. Most cardiac hemangiomas are asymptomatic, but large lesions are associated with exertional dyspnoea and may be considered for surgical resection. MRI can demonstrate the hypervascular nature of the hemangioma, which is suggestive for the diagnosis, classically they are isointense compared to myocardium on T1-weighted images due to slow flow and of diffuse high signal intensity on T2-weighted images. They enhance intensely with contrast in early phase, and may appear inhomogeneous depending upon the amount of fibrous tissue and interspersed calcification [33].

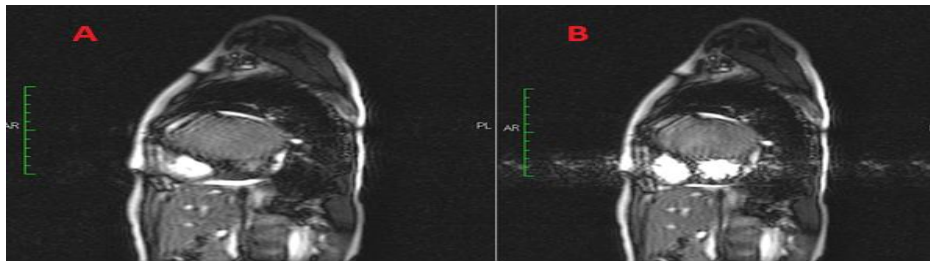


Fig-2: Cardiac MRI short axis view showing rhabdomyoma in a patient with tuberous sclerosis complex

D /fibroma

Cardiac fibromas are benign connective tissue tumors derived from fibroblasts that occur usually in children and constitute the second most common type (after the rhabdomyoma) of primary cardiac tumor occurring in the pediatric age group (34). Classically, they have an intramural location within the interventricular septum or left ventricular free wall [35]. They are often associated with arrhythmias which can be a presenting feature. They can also cause hemodynamic compromise and congestive heart failure. These tumors also may be found incidentally in asymptomatic patients [36]. On MRI fibromas are sharply demarcated and of uniformly low signal intensity compared with adjacent myocardium on both T1 and T2-weighted imaging due to their dense fibrous nature (37). A lack of first pass enhancement is typical, and LGE is commonly intense and uniform [38].

E/lipoma

Lipomas are well-encapsulated tumours usually composed of mature fat cells. True cardiac lipomas are much less frequent than lipomatous hypertrophy of the interatrial septum, but mostly arises from epicardial surface and can involve all three layers of heart. These tumors are usually incidental findings but secondary cardiac conduction disturbances and arrhythmias, including sudden death, are described [39]. On MRI appearances are typical owing to definitive characterization of fat signal which appears of uniformly high signal on both T1 and T2-weighted

imaging and fully suppresses with fat-saturated sequence. Due to their avascular nature there is no first pass or late gadolinium-enhanced with these lesions [40].

F/ teratoma

Teratoma is a germ cell tumor arising from all three germ cell layers, occurs in the pericardial cavity, and attaches to the root of the pulmonary artery and aorta or arising from atrial or ventricular wall protruding into cardiac chamber. Cardiac teratoma predominantly occur in children and young adults, and present with respiratory distress and cyanosis secondary to pericardial tamponade and compression of right sided vascular structures.

On CMR, teratomas demonstrate a large mass of heterogeneous signal intensity with areas of cysts, fat, soft tissue, and calcification; and so on the relationship of the tumor to the normal myocardium, great vessels, and other mediastinal structures can be better identified on CMR imaging [41].

G / rhabdomyoma :(figure 2)

Cardiac rhabdomyomas are myocardial hamartomas and are considered the most common fetal cardiac tumor frequently located in the myocardium of the ventricles, up to 50% occur in association with tuberous sclerosis [42]. The majority are asymptomatic, although they may be detected in utero because of autoimmune fetal hydrops and fatal death, other

presenting features include refractory arrhythmias left and ventricular outflow tract obstruction. On MRI, tumors have signal intensity that is similar to that of the adjacent myocardium on T1-weighted images and display relatively increased signal intensity on T2-weighted images [43].

H / paraganglioma

Paragangliomas are rare neuroendocrine tumors arising from the ganglia of the sympathetic or parasympathetic nervous system which tends to lie within the atrioventricular grooves and at the root of the great vessel origins [44]. Up to 50% of these tumours secrete catecholamines which explains the typical clinical presentation of headaches, palpitations, flushing, diaphoresis, and systemic arterial hypertension [3]. On magnetic resonance imaging these lesions classically range in size from 4-8 cm appearing well circumscribed. They are isointense to myocardium on T1 and usually show high signal intensity on T2-weighted images. First pass and late gadolinium enhanced is usually uniform and intense [46].

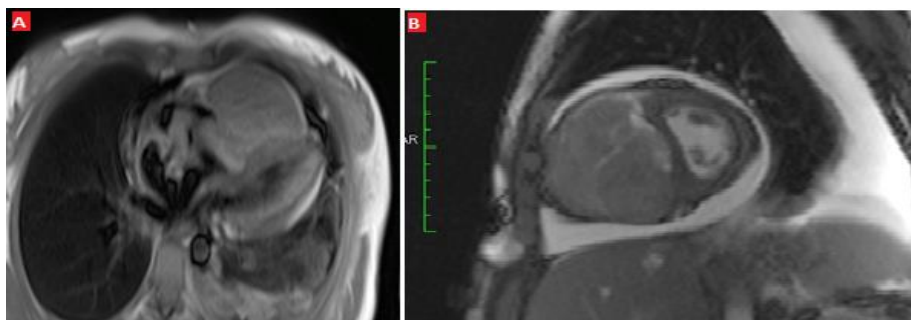


Fig-3: cardiac MRI short axis view demonstrating angiosarcoma

The MRI features of angiosarcoma include heterogeneous signal intensity originating from intratumoral hemorrhage and heterogeneous enhancement (48). Some unique characteristics include a polymorphic, “cauliflower” appearance on black-blood images, and a “sunray” aspect on enhanced MRI [49].

On steady-state free precession images, angiosarcoma is predominantly hyperintense relative to myocardium, with areas of high and low-signal intensity corresponding to hemorrhage and necrosis, respectively. Tubular structure with flow-void phenomenon may be seen due to the frequently large vascular channels [50].

Undifferentiated sarcoma

Undifferentiated sarcomas account for up to 25% of all primary cardiac tumors, results of immunohistochemical staining for multiple markers are usually negative, classically they arise within the left atrium and appear as a discrete infiltrative mass, generally along the posterior wall [51]. Signal intensity is isointense to myocardium on T1- and T2-weighted images with a heterogeneous enhancement pattern [52].

Malignant tumors

A/sarcoma

Sarcomas account for the majority of primary malignant cardiac tumors and are the second commonest primary tumor after myxoma. Histologically, they are classified into 3 main subgroups: angiosarcoma, sarcoma with myofibroblastic differentiation, and rhabdomyosarcoma.

Angiosarcoma: (figure 3)

Angiosarcomas are the most common malignant cardiac neoplasms, classically affects middle-aged men, the common place of angiosarcoma origination is the right atrium. Unfortunately, angiosarcomas are often asymptomatic until they become large and are associated with nonspecific cardiopulmonary symptoms related to the tumor size and infiltration. Metastases used to be developed in up to 80% patients at the moment of diagnosis. Most commonly, metastases are formed in the lungs, liver, lymph nodes, bone, brain adrenal glands, and spleen [47].

Leiomyosarcoma

A leiomyosarcoma is a rare malignant mesenchymal tumour arising from smooth muscle cell tissue. It has a predilection for the left atrium and often along its posterior wall with frequent infiltration into the pulmonary veins [53] causing dyspnoea, cardiac failure, peripheral embolism or atrial arrhythmias. MRI findings are infrequent, with intermediate signal to myocardium on T1-weighted images, and markedly increased signal intensity on T2-weighted black-blood images having been reported [54].

Fibrosarcoma

The primary fibrosarcoma of the heart is a rare tumor originating from the mesenchymal structures of the heart, these lesions originate within the left atrium in 50%, within either ventricle in 30% and from the pericardium in 20%. Symptoms are nonspecific with signs of right or left heart failure depending on localization. MRI findings are those of an infiltrative mass that classically has heterogeneous signal intensity on T1- and T2-weighted images.

Liposarcoma

Primary cardiac liposarcoma is an extremely rare tumor which is found in only about 1% of primary malignant cardiac tumors [55]. The majorities of these tumors originates from the right atrium and have also been reported to arise from the pericardium and valves. The symptoms are congestive heart failure, arrhythmia or arterial embolis, some present with cardiac tamponade [56]. On MRI, Necrosis and hemorrhage may be prominent, which can give them heterogeneous hyper-signal intensity on T1-weighted images [57].

Osteosarcoma

Primary cardiac osteosarcoma almost occurs in the left atrium and frequently involves the pulmonary vein ostia and mitral valve. They may have osteoblastic, chondroblastic, or fibroblastic differentiation. Macroscopic calcification is usually present, although calcification may not be readily apparent on CMRI as it appears as signal void on all sequences. As a result, they appear hypointense on T1- weighted sequences and hyperintense on T2-weighted images [58].

Rhabdomyosarcoma

Embryonal rhabdomyosarcoma is a common primary cardiac malignancy in infants and children, with slight male predelection. They involve the myocardium with equal prevalence in all

chambers. MRI descriptions are those of a large infiltrative mass with irregular margins and a tendency to central necrosis and cavitation. They are isointense on T1-weighted with central high signal on T2-weighted sequences [59]. The peripheral solid components frequently display homogeneous delayed enhancement [60].

Primary cardiac lymphoma: (figure 4)

Primary cardiac lymphoma (PCL) is a very rare disorder and is defined as disease confined to the heart or pericardium with no evidence of extracardiac disease [61]. Histologically, the majority of cases of PCL are diffuse B-cell lymphoma [62]. PCL occurs more usually in immunocompromised patients. The right atrium is the commonest site of origin with frequent involvement of more than 1 chamber and pericardial invasion. The most frequent cardiac clinical manifestations associated with PCL are pericardial effusion, heart failure, and atrioventricular block. On MRI, multiple nodular masses infiltrating through the myocardium, with a predilection for the right ventricle. Tumor nodules are usually iso or hyperintense relative to normal myocardium and demonstrate heterogeneous enhancement [63], diffuse pericardial infiltration in association with a hemorrhagic pericardial effusion can be seen [64].

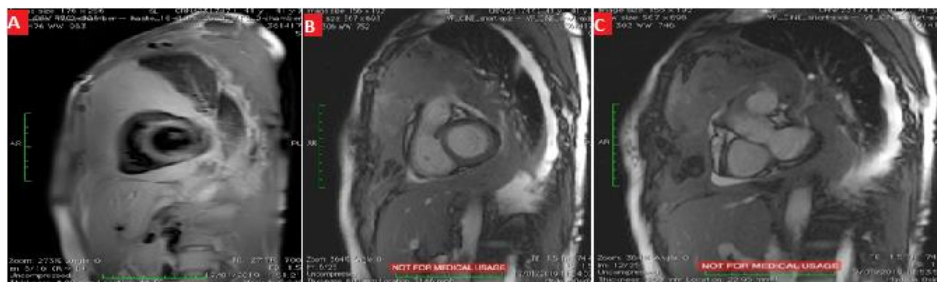


Fig-4: Cardiac MRI showing anterior mediastinum lymphoma infiltrating the pericardium.

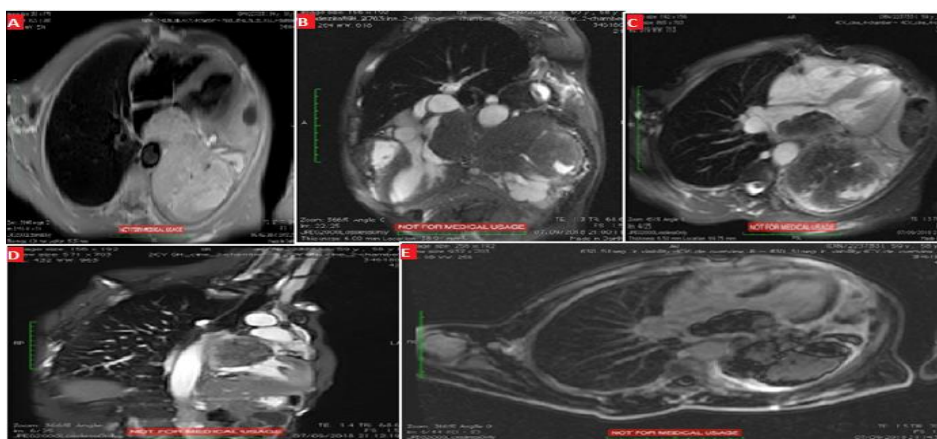


Fig-5: Cardiac MRI view demonstrating a locally advanced lung cancer invading the left atrium, the inferior wall of the left ventricle and the great vessels. Measuring 15cm / 10cm

Malignant metastatic tumors :(figure 5.6)

Metastases to the heart and pericardium are 40-50 times more frequent than primary cardiac tumors.

The incidence ranges from 2.3% to 18.3% [65]. They occur late in the course of a malignancy and isolated cardiac involvement is rarely seen without

dissemination to other organs. The pericardium is more frequently involved and typically manifest as a pericardial effusion causing progressive breathlessness and signs of tamponade. Hematogenous seeding is

classically the most common route of spread for tumors of bronchial and breast origin, followed by leukemia, melanoma and lymphoma [66].

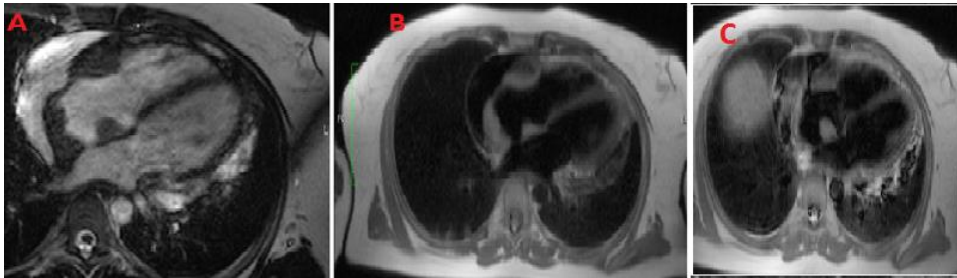


Fig-6: Cardiac MRI showing cardiac metastasis of a brain tumor invading the interventricular septum, the roof of the right atrium and right ventricle free wall

Transvenous cardiac extension to the right atrium via the inferior vena cava is typical of renal and hepatocellular carcinomas. MRI appearances of metastases are usually nonspecific and usually comprise enhancing masses or soft-tissue nodules. Melanoma has unique features owing to the T1 shortening properties of melanin and appears of hypersignal on T1-weighted images. A hemorrhagic pericardial effusion can be seen in association with metastases from any primary site.

Pericardial mesothelioma

Pericardial mesothelioma is a very rare malignant neoplasm derived from serous epithelial cells of the mesothelium. Although 50% of all primary pericardial tumors are pericardial mesotheliomas, they represent less than 1% of all malignant mesotheliomas. MRI showed homogeneous isointensity compared with myocardium on T1 and greater hyperintensity on T2 sequences. The tumor expands into the pericardial space compressing vessels and cardiac structures [67].

Pseudotumoral lesions

Intracardiac thrombus :(figure 7)

Thrombus is the major differential diagnosis for any intracardiac mass, especially atrial myxoma, with which it shares a common site of origin with particular predilection for the left atrial appendage. Other common locations are the left ventricle, especially in association with aneurysm formation post myocardial infarction, and the right atrium, when there is a central venous catheter. Signal characteristics of myxoma and thrombus overlap on MRI, although a multisequence evaluation with both dynamic rest perfusion and delayed enhancement images is often sufficient to confidently discriminate between these 2 entities. Signal intensity varies on T1- and T2-weighted images according to thrombus chronicity and contrast enhanced sequences are therefore more useful. Thrombus appears as a non enhancing low signal lesion on first pass perfusion and remains low signal on delayed enhancement images.

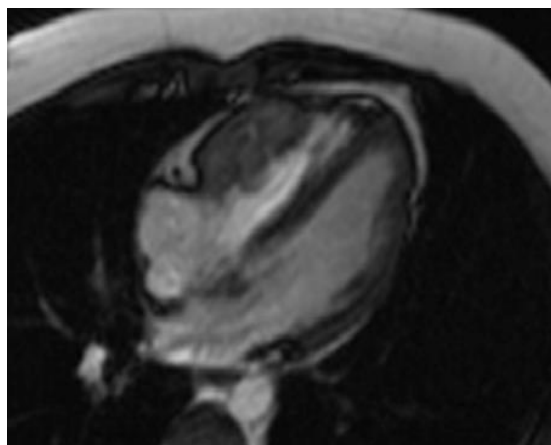


Fig-7: Cardiac MRI four chamber view showing thrombus in the lateral wall of the right ventricle in a patient with a medical history of Behçet's disease

Pericardial cyst

Pericardial cysts are benign congenital lesions that arise from the pericardium but do not communicate with the pericardial space. MRI Features are those of a fluid intensity lesion (low T1- and high T2-signal) that

does not enhance. Pericardial cyst may occasionally contain proteinaceous fluid and thus can have high signal intensity on T1 and T2-weighted sequences.

Bronchogenic cyst

Intracardiac Bronchogenic cysts are known as a rare tumor located in the atrioventricular septal region that may cause heart block [68], It is always misdiagnosed as the other intracardiac tumor, and definitive diagnosis should be made by pathology study. On MRI, bronchogenic cysts are sharply margined and usually rounded lesion that has variable signal intensity on T1-weighted images, dependent on

the amount of proteinaceous content, however, they show T2 hyperintensity with no evidence of late gadolinium enhancement.

Unusually, bacterial infection of the heart (mycobacterium, klebsiella, staphylococcus) parasitic (hydatid cyst) or fungal (aspergillosis) can display a similar image. (figure8)

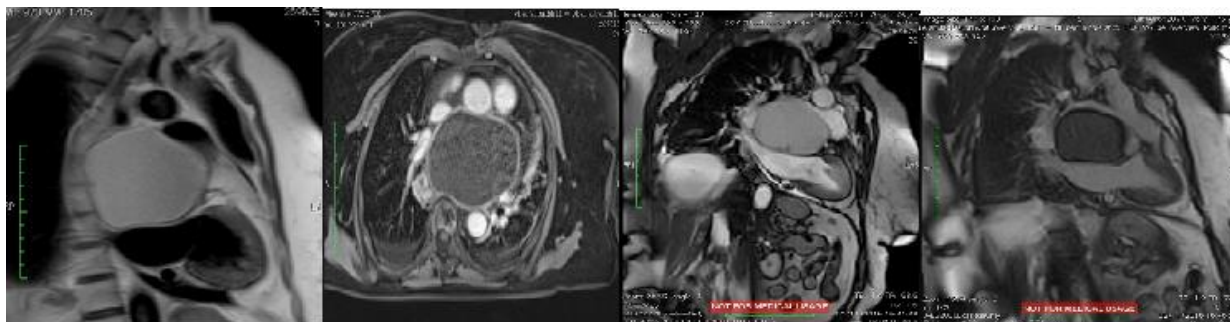


Fig-8: Cardiac MRI view demonstrating a large cardiac hydatid cyst measuring 94*70mm involving the aortic arch and compressing the left atrium

CONCLUSION

Cardiac tumors are rare; however, the differentiation of non-neoplastic lesions from neoplastic ones and a correct identification of the type of lesion is essential for appropriate therapeutic planning. Cardiac MRI is an important imaging modality for assessment of cardiac tumors because it enables non-invasive tissue characterization of tumors and determination of the extent of involvement and impact on cardiac flow and function.

REFERENCES

1. Roberts WC. Neoplasms involving the heart, their simulators, and adverse consequences of their therapy. *Proc (Bayl Univ Med Cent)*. 2001; 14:358-376.
2. Butany J, Nair V, Naseemuddin A, Nair GM, Catton C, Yau T. Cardiac tumours: diagnosis and management. *Lancet Oncol*. 2005; 6:219-228.
3. Peters PJ, Reinhardt S. The echocardiographic evaluation of intracardiac masses: a review. *J Am Soc Echocardiogr*. 2006; 19(2):230-40.
4. Altbach MI, Squire SW, Kudithipudi V, Castellano L, Sorrell VL. Cardiac MRI is complementary to echocardiography in the assessment of cardiac masses. *Echocardiography*. 2007; 24(3):286-300.
5. Sparrow PJ, Kurian JB, Jones TR, Sivananthan MU. MR imaging of cardiac tumors. *Radiographics*. 2005; 25(5):1255-76.
6. ElBardissi AW, Dearani JA, Daly RC, Mullany CJ, Orszulak TA, Puga FJ, Schaff HV. Survival after resection of primary cardiac tumors: a 48-year experience. *Circulation*. 2008 Sep 30; 118(14_suppl_1):S7-15.
7. Reynen K. Frequency of primary tumors of the heart. *Am J Cardiol*. 1996; 77(1):107.
8. Goodwin JF. The spectrum of cardiac tumors. *Am J Cardiol*. 1968; 21: 307-314.
9. Silverman NA. Primary cardiac tumors. *Ann Surg*. 1980; 191:127-138.
10. Bussani R, De-Giorgio F, Abbate A, Silvestri F. Cardiac metastases. *J Clin Pathol*. 2007; 60(1):27-34.
11. MacGee W. Metastatic and invasive tumors involving the heart in a geriatric population: a necropsy study. *Virchows Arch A Pathol Anat Histopathol*. 1991; 49(3):183-9.
12. Srichai MB, Junor C, Rodriguez LL, Stillman AE, Grimm RA, Lieber ML, Weaver JA, Smedira NG, White RD. Clinical, imaging, and pathological characteristics of left ventricular thrombus: a comparison of contrast-enhanced magnetic resonance imaging, transthoracic echocardiography, and transesophageal echocardiography with surgical or pathological validation. *American heart journal*. 2006 Jul 1; 152(1):75-84.
13. Dawson D, Mohiaddin R. Assessment of pericardial diseases and cardiac masses with cardiovascular magnetic resonance. *Prog Cardiovasc Dis*. 2011; 54(3):305-19.
14. Bakaeen FG, Reardon MJ, Coselli JS, Miller CC, Howell JF, Lawrie GM, Espada R, Ramchandani MK, Noon GP, Weilbaecher DG, DeBakey ME. Surgical outcome in 85 patients with primary cardiac tumors. *The American Journal of Surgery*. 2003 Dec 1; 186(6):641-7.
15. Donsbeck AV, Ranchere D, Coindre JM, Le Gall F, Cordier JF, Loire R. Primary cardiac sarcomas: an immunohistochemical and grading study with long-term follow-up of 24 cases. *Histopathology*. 1999; 34:295-304.

16. Shapira OM, Korach A, Izhar U, Koler T, Wald O, Ayman M, Erez E, Blackmon SH, Reardon MJ. Radical multidisciplinary approach to primary cardiac sarcomas. *European Journal of Cardio-Thoracic Surgery*. 2013 Feb 7;44(2):330-6.
17. Hundley WG, Bluemke DA, Finn JP, Flamm SD, Fogel MA, Friedrich MG, Ho VB, Jerosch-Herold M, Kramer CM, Manning WJ, Patel M. ACCF/ACR/AHA/NASCI/SCMR 2010 expert consensus document on cardiovascular magnetic resonance: a report of the American College of Cardiology Foundation Task Force on Expert Consensus Documents. *Journal of the American College of Cardiology*. 2010 Jun 8;55(23):2614-62.
18. Mitchell DG, Burk DL Jr, Vinitzki S, Rifkin MD. The biophysical basis of tissue contrast in extracranial MR imaging. *AJR Am J Roentgenol*. 1987;149:831-7.
19. Sparrow PJ, Kurian JB, Jones TR, Sivananthan MU. MR imaging of cardiac tumors. *Radiographics*. 2005;25:1255-76.
20. Simonetti OP, Finn JP, White RD, Laub G, Henry DA. "Black blood" T2-weighted inversion-recovery MR imaging of the heart. *Radiology*. 1996;199:49-57.
21. Hansen MW, Merchant N. MRI of hypertrophic cardiomyopathy: part I, MRI appearances. *AJR Am J Roentgenol*. 2007;189:1335-43.
22. Kramer CM, Barkhausen J, Flamm SD, Kim RJ, Nagel E; Society for Cardiovascular Magnetic Resonance Board of Trustees Task Force on Standardized Protocols. Standardized cardiovascular magnetic resonance imaging (CMR) protocols, society for cardiovascular magnetic resonance: board of trustees task force on standardized protocols. *J Cardiovasc Magn Reson*. 2008;10:35.
23. Hoffmann U, Globits S, Schima W, Loewe C, Puig S, Oberhuber G, Frank H. Usefulness of magnetic resonance imaging of cardiac and paracardiac masses. *Am J Cardiol*. 2003;92:890-5.
24. Kono T, Koide N, Hama Y, Kitahara H, Nakano H, Suzuki J, Isobe M, Amano J. Expression of vascular endothelial growth factor and angiogenesis in cardiac myxoma: a study of fifteen patients. *J Thorac Cardiovasc Surg*. 2000;119:101-7.
25. Eckhardt BP, Dommann-Scherrer CC, Stuckmann G, Zollikofer CL, Wentz KU. Giant cardiac myxoma with malignant transformed glandular structures. *Eur Radiol*. 2003;13:2099-102.
26. Keeling IM, Oberwalder P, Anelli-Monti M, Schuchlenz H, Demel U, Tilz GP, Rehak P, Rigler B. Cardiac myxomas: 24 years of experience in 49 patients. *European Journal of Cardio-Thoracic Surgery*. 2002 Dec 1;22(6):971-7.
27. Sparrow PJ, Kurian JB, Jones TR, Sivananthan MU. MR imaging of cardiac tumors. *Radiographics*. 2005;25:1255-76.
28. Bruce CJ. Cardiac tumours: diagnosis and management. *Heart*. 2011;97:151-60.
29. Grebenc ML, Rosado-de-Christenson ML, Green CE, Burke AP, Galvin JR. Cardiac myxoma: imaging features in 83 patients. *Radiographics*. 2002; 22: 673-89.
30. Van Werkum MH, Swaans MJ, van Es HW, Rensing B, van Heesewijk JP. Case 190: papillary fibroelastoma of the pulmonary valve. *Radiology*. 2013 Feb;266(2):680-4.
31. Kondruweit M, Schmid M, Strecker T. Papillary fibroelastoma of the mitral valve: appearance in 64-slice spiral computed tomography, magnetic resonance imaging, and echocardiography. *European heart journal*. 2007 Oct 24;29(6):831-.
32. Grebenc ML, Rosado de Christenson ML, Burke AP, Green CE, Galvin JR. Primary cardiac and pericardial neoplasms: radiologic-pathologic correlation. *Radiographics*. 2000 Jul;20(4):1073-103.
33. Oshima H, Hara M, Kono T, Shibamoto Y, Mishima A, Akita S. Cardiac hemangioma of the left atrial appendage: CT and MR findings. *Journal of thoracic imaging*. 2003 Jul 1;18(3):204-6.
34. Gow RM, Haney I, Mawson J, Williams WG, Freedom RM. Pediatric primary benign cardiac tumors: a 15-year review. *American heart journal*. 1997 Dec 1;134(6):1107-14.
35. ElBardissi AW, Dearani JA, Daly RC, Mullany CJ, Orszulak TA, Puga FJ, Schaff HV. Analysis of benign ventricular tumors: long-term outcome after resection. *The Journal of thoracic and cardiovascular surgery*. 2008 May 1;135(5):1061-8.
36. Herman TE, Siegel MJ, McAlister WH. Cardiac tumor in Gorlin syndrome. *Pediatric radiology*. 1991 Apr 1;21(3):234-5.
37. Brechtel K, Reddy GP, Higgins CB. Cardiac fibroma in an infant: magnetic resonance imaging characteristics. *Journal of Cardiovascular Magnetic Resonance*. 1999 Jan 1;1(2):159-61.
38. O'Donnell DH, Abbara S, Chaitiraphan V, Yared K, Killen RP, Cury RC, Dodd JD. Cardiac tumors: optimal cardiac MR sequences and spectrum of imaging appearances. *American Journal of Roentgenology*. 2009 Aug;193(2):377-87.
39. Friedberg MK, Chang IL, Silverman NH, Ramamoorthy C, Chan FP. Images in cardiovascular medicine. Near sudden death from cardiac lipoma in an adolescent. *Circulation*. 2006;113:e778-9.
40. Restrepo CS, Largoza A, Lemos DF, Diethelm L, Koshy P, Castillo P, Gomez R, Moncada R, Pandit M. CT and MR imaging findings of benign cardiac tumors. *Curr Probl Diagn Radiol*. 2005;34:12-21.
41. Beghetti M, Prieditis M, Rebeyka IM, Mawson J. Images in cardiovascular medicine. Intrapericardial teratoma. *Circulation*. 1998 ;97 :1523-1524.
42. Gow RM, Haney I, Mawson J, Williams WG, Freedom RM. Pediatric primary benign cardiac

- tumors: a 15-year review. *American heart journal*. 1997 Dec 1;134(6):1107-14.
43. Christophe C, Bartholome J, Blum D, Clerckx A, Desprechins B, De Wolf D, Gallez A, Viart P, Perlmutter N. Neonatal tuberous sclerosis. *Pediatric radiology*. 1989 Jul 1;19(6-7):446-8.
 44. Reynen K. Cardiac myxomas. *New England Journal of Medicine*. 1995 Dec 14;333(24):1610-7.
 45. Wang JG, Han J, Jiang T, Li YJ. Cardiac paragangliomas. *J Card Surg*. 2015;30(1):55–60.
 46. Manger WM. An overview of pheochromocytoma: history, current concepts, vagaries, and diagnostic challenges. *Annals of the New York Academy of Sciences*. 2006 Aug;1073(1):1-20.
 47. Patel SD, Peterson A, Bartczak A, Lee S, Chojnowski S, Gajewski P, Loukas M. Primary cardiac angiosarcoma—a review. *Medical science monitor: international medical journal of experimental and clinical research*. 2014;20:103.
 48. Pigott C, Welker M, Khosla P, Higgins RS. Improved outcome with multimodality therapy in primary cardiac angiosarcoma. *Nature Reviews Clinical Oncology*. 2008 Feb;5(2):112.
 49. Yahata S, Endo T, Honma H, Ino T, Hayakawa H, Ogawa M, Hayashi H, Kumazaki T. Sunray appearance on enhanced magnetic resonance image of cardiac angiosarcoma with pericardial obliteration. *American heart journal*. 1994 Feb 1;127(2):468-71.
 50. Deetjen AG, Conradi G, Möllmann S, Hamm CW, Dill T. Cardiac angiosarcoma diagnosed and characterized by cardiac magnetic resonance imaging. *Cardiology in review*. 2006 Mar 1;14(2):101-3.
 51. Itoh K, Matsumura T, Egawa Y, Watanabe M, Ohshio T, Ohta A, Hayabuchi Y, Seki K. Primary mitral valve sarcoma in infancy. *Pediatric cardiology*. 1998 Mar 1;19(2):174-7.
 52. Arazo PA, Eklund HE, Welch TJ, Breen JF. CT and MR imaging of primary cardiac malignancies. *Radiographics*. 1999 Nov;19(6):1421-34.
 53. Clarke NR, Mohiaddin RH, Westaby S, Banning AP. Multifocal cardiac leiomyosarcoma. Diagnosis and surveillance by transoesophageal echocardiography and contrast enhanced cardiovascular magnetic resonance. *Postgraduate medical journal*. 2002 Aug 1;78(922):492-3.
 54. Lo FL, Chou YH, Tiu CM, Lan GY, Hwang JH, Chern MS, Teng MM. Primary cardiac leiomyosarcoma: imaging with 2-D echocardiography, electron beam CT and 1.5-Tesla MR. *European journal of radiology*. 1998 Mar 1;27(1):72-6.
 55. Kitamura A, Ozaki N, Mukohara N, Yoshida M, Shida T. Primary cardiac liposarcoma causing cardiac tamponade: report of a case. *Surgery today*. 2007 Nov 1;37(11):974-6.
 56. Kitamura A, Ozaki N, Mukohara N, Yoshida M, Shida T. Primary cardiac liposarcoma causing cardiac tamponade: report of a case. *Surgery today*. 2007 Nov 1;37(11):974-6.
 57. Schrem SS, Colvin SB, Weinreb JC, Glassman E, Kronzon I. Metastatic cardiac liposarcoma: diagnosis by transesophageal echocardiography and magnetic resonance imaging. *Journal of the American Society of Echocardiography*. 1990 Mar 1;3(2):149-53.
 58. Yamagishi M, Yamada N, Kuribayashi S. Images in cardiology: Magnetic resonance imaging of cardiac osteosarcoma. *Heart*. 2001;85:311.
 59. Gilkeson RC, Chiles C. MR evaluation of cardiac and pericardial malignancy. *Magn Reson Imaging Clin N Am*. 2003; 1:173-86.
 60. Villacampa VM, Villarreal M, Ros LH, et al. Cardiac rhabdomyosarcoma: Diagnosis by MR imaging. *Eur Radiol*. 1999;9:634-7.
 61. Burke A. Primary malignant cardiac tumors. *Semin Diagn Pathol*. 2008;25:39-46.
 62. Ceresoli GL, Ferreri AJ, Bucci E, Ripa C, Ponzoni M, Villa E. Primary cardiac lymphoma in immunocompetent patients: diagnostic and therapeutic management. *Cancer: Interdisciplinary International Journal of the American Cancer Society*. 1997 Oct 15;80(8):1497-506.
 63. Ryu SJ, Choi BW, Choe KO. CT and MR findings of primary cardiac lymphoma: report upon 2 cases and review. *Yonsei medical journal*. 2001 Aug 1;42(4):451-6.
 64. Chiles C, Woodard PK, Gutierrez FR, Link KM. Metastatic involvement of the heart and pericardium: CT and MR imaging. *Radiographics*. 2001 Mar;21(2):439-49.
 65. Bussani R, De-Giorgio F, Abbate A, Silvestri F. Cardiac metastases. *Journal of clinical pathology*. 2007 Jan 1;60(1):27-34.
 66. Hancock EW. Neoplastic pericardial disease. *Cardiology clinics*. 1990 Nov 1;8(4):673-82.
 67. Kaminaga T, Yamada N, Imakita S, Takamiya M, Nishimura T. Magnetic resonance imaging of pericardial malignant mesothelioma. *Magnetic resonance imaging*. 1993 Jan 1;11(7):1057-61.
 68. Travers H. Congenital polycystic tumor of the atrioventricular node: possible familial occurrence and critical review of reported cases with special emphasis on histogenesis. *Human pathology*. 1982 Jan 1;13(1):25-35.